NASA Contractor Report 191196

Thermomechanical and Isothermal Fatigue Behavior of a $[90]_8$ Titanium Matrix Composite

Michael G. Castelli
Sverdrup Technology, Inc.
Lewis Research Center Group
Brook Park, Ohio

Prepared for the
Eighth Technical Conference on Composite Materials
sponsored by the American Society for Composites
Cleveland, Ohio, October 19–21, 1993

Prepared for
Lewis Research Center
Under Contract NAS3–25266

NASA
National Aeronautics and
Space Administration

THERMOMECHANICAL AND ISOTHERMAL FATIGUE BEHAVIOR OF A $[90]_8$ TITANIUM MATRIX COMPOSITE

Michael G. Castelli
Sverdrup Technology, Inc.
Lewis Research Center Group
Brook Park, Ohio, 44142

Abstract

An experimental investigation was conducted to analyze the fatigue damage mechanisms operative in a 35 fiber volume percent [90°] titanium matrix composite (TMC) under 427°C isothermal and thermomechanical loading conditions. The thermomechanical fatigue (TMF) tests were performed with a temperature cycle from 200 to 427°C under closely controlled conditions to define both the deformation and fatigue life behavior. Degradation of the TMC's isothermal elastic moduli and coefficient of thermal expansion were monitored throughout the TMF tests. The results indicated TMF life trends which contrasted those established in a comparable [0°] system, as TMF loading of the [90°] TMC was not found to be "life-limiting" in comparison to maximum temperature isothermal conditions. In-phase lives were very similar to those established under 427°C isothermal conditions. High stress isothermal fatigue at 427°C produced increased strain ratchetting and stiffness degradation relative to TMF conditions. Out-of-phase loadings produced TMF lives approximately an order of magnitude greater than the lives determined under isothermal and in-phase conditions. Extensive fractography and metallography were also performed. Two key issues were identified and appeared to dominate the fatigue damage and life of the [90°] TMC, namely, 1) the weak fiber/matrix interface, and 2) environmental attack of the fiber/matrix interface via the exposed [90°] fiber ends.

Introduction

Titanium matrix composites (TMCs) are currently being developed and investigated for a number of high-temperature airframe and propulsion system applications. In many such applications, materials will experience a variety of multiaxial loads, thus, establishing a requirement for the material to be capable of carrying loads in more than one primary direction. Therefore, many composite materials will necessarily incorporate multiple fiber orientations, the most obvious of which include the [0°] and [90°] directions, where [0°] indicates fibers parallel to, and [90°] indicates fibers perpendicular to the loading direction.

High temperature testing of various TMCs containing [90°] fibers has revealed that the fatigue properties are drastically reduced from those exhibited by the unidirectional [0°] systems (Gayda and Gabb, 1992; Lerch and Saltsman, 1991; Majumdar and Newaz, 1991 and 1992; Pollock and Johnson, 1992). Much of this degradation has been attributed to the weak bond at the fiber/matrix (F/M) interface, which appears to either fail at extremely low stresses, or is essentially non-existent beyond that which is mechanically induced by tensile residual stresses in the matrix. This raises obvious questions concerning the performance of a [90°] TMC under thermomechanical loading conditions, particularly in light of the dramatic fatigue-life reductions which can occur in a [0°] TMC when thermomechanical fatigue (TMF) conditions are introduced (Castelli et al., 1992).

The work presented here was undertaken to characterize the isothermal and thermomechanical deformation, damage, and fatigue life behaviors of a [90°] TMC. Differences in material deformation and cyclic fatigue life are noted as functions of cycle type. Also, damage progressions as indicated by the changes in composite stiffness and coefficient of thermal expansion (CTE) are discussed and compared for the various cycle types. Fractographic and metallographic investigations are also used to assist in defining the damage mechanisms.

Material and Test Details

The TMC used for this study consisted of Ti-15V-3Cr-3Al-3Sn (weight percent) alloy matrix reinforced with approximately 35 volume percent (v/o) of continuous SiC (SCS-6) fibers. The SCS-6 fiber has a nominal diameter of 140 μm. All composite test specimens were obtained from a single eight-ply unidirectionally reinforced panel fabricated by HIPing alternate layers of Ti-15-3 foil and SCS-6 fiber mat. The resulting panel thickness was approximately 2 mm.

A dogbone-shaped coupon specimen geometry was utilized (Worthem, 1990) featuring a radius cut of 36.8 cm and a nominal geometry of 15.2 x 1.3 cm. This specimen geometry provided for consistent parallel section failures, producing satisfactory results for all isothermal fatigue and TMF tests. Test specimens were cut from the composite panel by means of wire electro-discharge machining (EDM); subsequently, a light diamond wheel grind was used to remove the heat-affected zone. Given that the Ti-15-3 is a metastable alloy, all specimens were heat treated at 700°C for 24 hours in vacuum to stabilize the microstructure.

A series of zero-tension (R_σ=0), load-controlled isothermal and TMF tests were performed in air. All tests employed direct induction heating, triangular waveforms for the control variables, and a cyclic load period of 2 minutes (frequency = $8.3x10^{-3}$ Hz). Axial strain measurements were made with a high temperature extensometer mounted on the edge of the specimen. The isothermal tests were conducted at a temperature of 427°C. Load/temperature 0° in-phase and 90° out-of-phase (IP and OP, respectively) TMF cycles were performed with a temperature cycle from 200 to 427°C. Specimen cooling was achieved through a combination of cold grips and forced air. However, the forced air was maintained to an absolute minimum to allow for a high degree of temperature gradient control over the specimen's test section.

The TMF test technique used in this study (Castelli, 1993) to quantify both the stiffness and the CTE degradations during TMF testing is shown graphically in Fig. 1. After each TMF cycle designated for data collection, the specimen is subjected to a thermal cycle under zero load, represented by the horizontal line from T_1 to T_2. This thermal cycle allows the real-time or "current" thermal strain characteristics of the composite to be explicitly measured with the high temperature extensometer. At the extremes of the thermal cycle (i.e. 200 and 427°C), the temperatures are briefly stabilized and small elastic loads are applied; these loadings are represented by the stress-strain lines marked E_1 and E_2 on Fig. 1. This allows explicit measurements of the material's "current" isothermal stiffness values at both temperature extremes.

There are several benefits realized from this technique. First, the "real-time" thermal strain information is essential for an accurate post-test assessment of the mechanical strain response. Second, the CTE and isothermal moduli (E) measurements provide a definitive quantitative measurement for tracking the TMF damage progression. Third, measurement of the isothermal E values enables direct stiffness degradation/damage comparisons between TMF and isothermal fatigue loadings.

In comparison to a conventional TMF test, this technique introduces several additional thermal cycles at zero load and several relatively small elastic loads. These additional loadings were found to be inconsequential with respect to the ongoing material damage and resulting TMF life. This was verified throughout the development and implementation of the test technique (Castelli, 1993).

Results and Discussion

Fatigue Life Behavior

Prior to discussing the [90°] TMC behavior, it is worthwhile to briefly review the general TMF life trends of the [0°] TMC for subsequent comparisons. This information is given in Fig. 2 for zero-tension TMF with a temperature cycle of 93 to 538°C (Castelli et al., 1992). The IP and OP TMF conditions were found to be life-limiting, relative to isothermal conditions, for all of the stress levels investigated. At relatively high maximum stress (S_{max}) levels, IP loadings promoted accelerated strain ratchetting and enhanced the mechanism of load shedding from the matrix to the fibers. This resulted in extremely short cyclic lives and eventual tensile overload failures associated with extensive

fiber cracking and little or no observable matrix damage. As the S_{max} levels decreased, the IP and OP TMF life curves crossed and established the life regime where OP conditions became life-limiting. The OP TMF damage mechanisms were significantly different from those dominating under IP TMF conditions. The OP loadings produced environment enhanced matrix cracking initiated at surface and near-surface locations. This matrix dominated damage was typically present in the absence of fiber cracking.

The 427°C isothermal and 200 to 427°C TMF life results are shown on a stress basis for the $[90°]_8$ TMC in Fig. 3. Note the significant loss in fatigue resistance from the [0°] TMC to the [90°] TMC by noting the stress levels in Figs. 2 and 3. Cyclic lives resulting from IP TMF were very similar to those produced under isothermal conditions, even at relatively high levels of S_{max}. However, the lives exhibited under OP TMF were consistently greater than the isothermal and IP TMF lives by approximately an order of magnitude. It is obvious that these fatigue life trends are inconsistent with those displayed by the [0°] TMC (Castelli et al., 1992). Further discussion will show that the mechanisms leading to reduced [0°] TMF lives relative to isothermal lives, such as load shedding under IP conditions and extensive surface cracking under OP conditions, are either non-existent or ineffectual in the [90°] system because of the extremely weak F/M bond.

Fig. 4 is a plot of several of these data on a strain range basis. The strain range values used were those existing at ½ the number of cycles to failure ($½N_f$). Also shown are Ti-15-3 matrix fatigue data generated at 427°C under strain control with R_ε=0 (Castelli and Gayda, 1993). By comparing the lives in this fashion we see that all of the data collapse quite well. Note, however, the dramatic life reduction between the various [90°] data and the 427°C isothermal fiberless Ti-15-3 data. This notable reduction is also evident on a stress range basis.

Isothermal Deformation and Damage

The deformation response under isothermal conditions with S_{max}=150 MPa is shown in Fig. 5. In comparison to subsequent cycles, the first cycle revealed a significant degree of inelastic behavior. This nonlinear response results predominantly from F/M de-bonding, and with increasing stress, plastic flow of the matrix. One form of damage to note was the overall strain ratchetting which occurred over the course of a test. The strain ratchetting is enabled due to the load-control nature of the test and clearly increased with increasing applied S_{max}. The representative test shown in Fig. 5 reveals an accumulated "permanent" strain (at zero load) of 0.01 m/m at cycle 1000 (0.75 N_f). All isothermal tests exhibited notable increases in both peak strain and strain range with continued cycling. These increases are believed to be chiefly associated with additional F/M interface damage and propagation of fatigue cracks from the interfaces. It is also likely that matrix creep contributed to the strain accumulation.

Another measure of composite damage was stiffness degradation. Fig. 6 traces the degradation of the 427°C static unloading modulus as a function of accumulated isothermal fatigue cycles; four tests are shown. Tests where S_{max} was less than 150 MPa revealed a measurable but small drop in static modulus after the first cycle. In contrast, the S_{max}=150 and 220 MPa tests experienced extensive first-cycle damage, as moduli decreases of 32 and 60 percent, respectively, were experienced. Note that these initial stiffness drops were primarily related to various states of F/M de-bonding and interface damage, as opposed to stages of fatigue cracking which accumulates later in cyclic life. Two features detailed in the modulus degradation curves are clearly worth noting. First, the stiffness values for all of the tests tended to converge to the same magnitude, irrespective of the first-cycle damage or the cyclic stress level. The specimens which sustained large first-cycle stiffness drops exhibited reduced subsequent cyclic stiffness degradations. Convergence of the stiffness values occurred at approximately 200 cycles (The S_{max}=220 MPa test failed at N=166.) with a value of approximately 50 GPa. Note that this value corresponds with that exhibited after the first-cycle damage in the S_{max}=220 MPa test, and may be indicative of a fully degraded F/M interface, with continued stiffness degradation primarily representing that resulting from fatigue crack growth.

The second feature to note from Fig. 6 was the increase in static moduli experienced from approximately 200 to 3000 cycles. This stiffening trend was most likely caused by the microstructural precipitation of an α-Ti phase in the metastable Ti-15-3 matrix. Precipitation of this phase has been noted to promote both stiffening and dramatic microstructural hardening effects (Lerch et al., 1990). Although considerable crack propagation, and thus damage progression, is likely occurring over this cyclic range, the damage progression is not detectable in the form of a static modulus decrease because of the overriding stiffening effect of the α-phase precipitation.

Thermomechanical Deformation and Damage

Deformation responses experienced under IP and OP TMF conditions with S_{max}=150 MPa are given in Figs. 7 and 8, respectively. The loops are shown in terms of mechanical strain, where the thermal strain component has been subtracted out. Recall that the thermal strain component was not assumed to remain constant, but rather it was measured at each recorded cycle, allowing for accurate assessments of the mechanical strain components. The IP test experiences a degree of strain ratchetting that is comparable to but slightly less than that experienced during isothermal loading. This trend was typical at other levels of S_{max} and appears to have been associated with the comparable life trends established between the IP and isothermal loadings. In contrast, the OP test experienced only 40 percent of the ratchetting which occurred during the IP test. This trend was generally expected, given that the maximum load occurred at 200°C, as opposed to 427°C, which was the case for the IP and isothermal cycles.

Stiffness degradations as functions of TMF damage were monitored by explicitly measuring the isothermal moduli at 200 and 427°C for each data collection cycle. The moduli values are plotted in Fig. 9 for the tests shown in Figs. 7 and 8. The first-cycle degradation was comparable for both the IP and OP loadings. However, the IP test moduli began to degrade much earlier in cyclic life; this was in agreement with the fatigue life behaviors and reveals that the IP cycle was considerably more damaging. Note that for both IP and OP conditions the moduli at 427°C began to degrade prior to those measured at 200°C. This may have been indicative of cracks opening at the higher temperatures and also related to the state of residual stresses in the specimen. By comparing the first-cycle stiffness degradation experienced in the TMF tests (≈ 10 percent change) to that in the isothermal test with S_{max}=150 MPa (32 percent change) it appears that the isothermal loading was more damaging. Also note that the increases in moduli observed over the range of 200 to 3000 cycles during isothermal loadings were not observed in the TMF tests. This may be expected, given that the isothermal tests were continually exposed to the maximum temperature of the TMF cycle, enhancing conditions for precipitation of the α-Ti phase.

Degradations of the composite's mean CTEs for the S_{max}=150 MPa IP and OP TMF tests are shown in Fig. 10. This value was defined as the change in thermal strain from 200 to 427°C divided by the change in temperature; that is, $\Delta\varepsilon^{th}$/227°C. As TMF damage accumulated in the composite, the mean CTE in the [90°] direction increased. Although this result is somewhat surprising at first, it can be easily understood by examining a simple expression for the composite CTE in the [90°] or "transverse" direction (CTE_T). Schapery (1968) has derived the expression for CTE_T, yielding:

$$CTE_T = (1 + \nu_f)\, CTE_f\, V_f + (1 + \nu_m)\, CTE_m\, V_m - CTE_L\, \nu_L$$

where ν and V are Poisson's ratio and volume fraction, respectively, and subscripts f, m, and L represent the fiber, matrix, and composite longitudinal direction, respectively. If the ensuing damage introduces a decrease in restraint along the composite's longitudinal direction (the last term), it can be seen from the equation above that the CTE_T will increase. Previous experimental results on a longitudinally reinforced TMC clearly reveal that both the CTE_L and E_L decrease with ensuing TMF

damage where matrix cracking is present (Castelli, 1993). In light of this result, and considering the present condition of extensive F/M de-bonding and fatigue cracking from the F/M interfaces, the increasing CTE_T trends are explicitly supported. Also note that the increases in CTE_T shown in Fig. 10 directly correspond to the decreases in transverse stiffness shown in Fig. 9.

Fractography and Metallography

Representative scanning electron microscope (SEM) fractographs are shown in Figs. 11 and 12 from IP and OP TMF specimens, respectively. No failure mechanisms were found to be unique to any one cycle type. This again is in direct contrast to the trends established in the [0°] TMC system, where distinct differences were noted (Castelli et al., 1992). All [90°] fractographs revealed exclusive internal crack initiations at F/M interface locations. Oxidized matrix fatigue cracking dominated all of the fracture surfaces. The extent of oxidation at surface locations was modest in comparison to that which occurred at internal cracked matrix locations. The exposed [90°] fibers along the specimen's cut edges appeared to serve as oxygen "pipelines" to the numerous cracks which were propagating at the interfaces.

Moderate to low stress isothermal and IP TMF specimens, such as the one shown in Fig. 11, revealed the most extensive cracking with very little matrix area exhibiting ductile/tensile failure. Also note the relatively high number of individual cracks which are evident in Fig. 11, suggesting a high number of initiation points. Fig. 12 reveals a fracture surface generated from a higher S_{max} OP TMF loading condition. Here, as in Fig. 11, multiple fatigue cracks were initiated at the F/M interfaces. However, the extent of matrix cracking was not as "mature" as that shown in Fig. 11 because the greater S_{max} promoted a tensile overload failure before complete "through-the-thickness" transverse cracking could occur. Thus, distinct "strips" exhibiting ductile microvoid coalescence were often created along approximate centerlines of the matrix layers during the final tensile failure event. Similar features were also evident under relatively high stress isothermal and IP TMF conditions.

SEM fractography also revealed that the regions of flat fatigue cracking in the matrix often coincided with F/M interface locations where the bond appeared to remain intact, transverse to the loading direction. In other words, if the fiber cross-section were considered as a clock face and the uniaxial loading was in the 12 and 6 o'clock directions, the bond being referred to here is at the 3 and 9 o'clock positions. Locations where de-bonding occurred at these 3 and 9 o'clock positions were typically associated with ductile failure in the adjacent matrix; this trend is clearly illustrated in the SEM fractography shown in Fig. 13.

Metallographic mounts were examined from both longitudinal and transverse sections; representative sections from longitudinal cuts through the specimen's thickness are shown in Figs. 13 and 14. All mounts revealed damage consistent with observations made from the fracture surfaces. No surface matrix cracking or fiber splitting, and minimal transverse fiber cracking was evident. Extensive F/M de-bonding, such as that shown in Fig. 14, was clearly visible. The majority of fibers exhibited cracks initiated at the F/M interface locations. Using the clock face analogy described above with the loading direction representing 6 and 12 o'clock, the vast majority of cracks initiated between the 2 to 4 and 8 to 10 o'clock positions, and propagated transverse to the loading direction into the matrix; see Fig. 14. Fig. 15 reveals a fiber where the F/M interface is clearly de-bonded in the loading direction, but the bond appears to have remained intact at approximately the 9 (below the transverse crack) and 3 o'clock positions. This occurrence is synonymous with that which is described on the fracture surface shown in Fig. 13.

Summary

In contrast to the trends established in the [0°] titanium matrix composite (TMC) system, zero-tension in-phase (IP) and out-of-phase (OP) thermomechanical fatigue (TMF) conditions were not found to be "life-limiting" in the [90°] system. Isothermal fatigue loadings at representative maximum temperatures were determined to be most damaging. This was evidenced by increased strain

ratchetting and stiffness degradation relative to the TMF loadings. However, IP TMF lives were only slightly greater than those established under maximum temperature isothermal conditions. The OP TMF lives were consistently greater than isothermal and IP TMF lives by an order of magnitude. No failure mechanisms were found to be unique to any one cycle type, as all were found to be dominated by fiber/matrix (F/M) de-bonding and environment assisted matrix fatigue cracking initiated at F/M interfaces. The first-cycle de-bonding immediately introduces a significant degree of damage in the composite. Thus, resulting cyclic fatigue lives are primarily related to the characteristics of fatigue crack growth in the matrix material.

Two key issues appear to dominate the fatigue damage and greatly reduced fatigue life properties of TMCs containing [90°] fibers, namely,

1) the weak fiber/matrix interface, and

2) environmental attack of the fiber/matrix interface via exposed [90°] fiber ends.

Acknowledgements

The author wishes to acknowledge Rod Ellis for his support and input to this research and Chris Burke, Ralph Corner, and Ron Shinn for their technical assistance in the Fatigue and Structures Laboratory and the Metallographic Laboratory at NASA Lewis Research Center.

References

Castelli, M.G., 1993, "An Advanced Test Technique to Quantify Thermomechanical Fatigue Damage Accumulation in Composite Materials," NASA CR-191147, NASA Lewis Research Center, Cleveland, OH.

Castelli, M.G., Bartolotta, P.A. and Ellis, J.R., 1992, "Thermomechanical Testing of High-Temperature Composites: Thermomechanical Fatigue Behavior of SiC(SCS-6)/Ti-15-3," *Composite Materials: Testing and Design (Tenth Volume), ASTM STP 1120*, Glen C. Grimes, Ed., Philadelphia, PA, pp. 70-86.

Castelli, M.G. and Gayda, J., 1993, "An Overview of Elevated Temperature Damage Mechanisms and Fatigue Behavior of a Unidirectional SCS-6/Ti-15-3 Composite," DE-Vol. 55, *Reliability, Stress Analysis, and Failure Prevention*, ASME, September, 1993, pp. 213-221.

Gabb, T.P., Gayda, J. and MacKay, R.A., 1990, "Isothermal and Nonisothermal Fatigue Behavior of a Metal Matrix Composite," *J. of Composite Materials*, Vol 24, June, pp. 667-686.

Gayda, J. and Gabb, T.P., 1992, "Isothermal Fatigue Behavior of a $[90]_8$ SiC/Ti-15-3 Composite at 426°C," *Int. J. of Fatigue*, Jan., pp. 14-20.

Lerch, B.A., Gabb, T.P. and MacKay, R.A., 1990, "Heat Treatment of the SiC/Ti-15-3 Composite System," NASA TP-2970, NASA Lewis Research Center, Cleveland, OH.

Lerch, B.A. and Saltsman, J.F., 1991, "Tensile Deformation and Damage in SiC Reinforced Ti-15V-3Cr-3Al-3Sn," NASA TM-103620, NASA Lewis Research Center, Cleveland, OH.

Majumdar, B.S. and Newaz, G.M., 1991, "Thermomechanical Fatigue of a Quasi-Isotropic Metal Matrix Composite," *Composite Materials: Fatigue and Fracture (Third Volume), ASTM STP 1110*, T. Kevin O'Brien, Ed., Philadelphia, pp. 732-752.

Majumdar, B.S. and Newaz, G.M., 1992, "Inelastic Deformation of Metal Matrix Composites: Plasticity and Damage Mechanisms - Part II," NASA TM-189096, NASA Lewis Research Center, Cleveland, OH.

Pollock, W.D. and Johnson, W.S., 1992, "Characterization of Unnotched SCS-6)/Ti-15-3 Metal Matrix Composites at 650°C," *Composite Materials: Testing and Design (Tenth Volume), ASTM STP 1120*, Glen C. Grimes, Ed., Philadelphia, pp. 175-191.

Schapery, R.A., 1968, "Thermal Expansion Coefficients of Composite Materials Based on Energy Principles," *J. of Composite Materials*, Vol 2, pp. 380-404.

Worthem, D.W., 1990, "Flat Tensile Specimen Design for Advanced Composites," NASA CR-185261, NASA Lewis Research Center, Cleveland, OH.

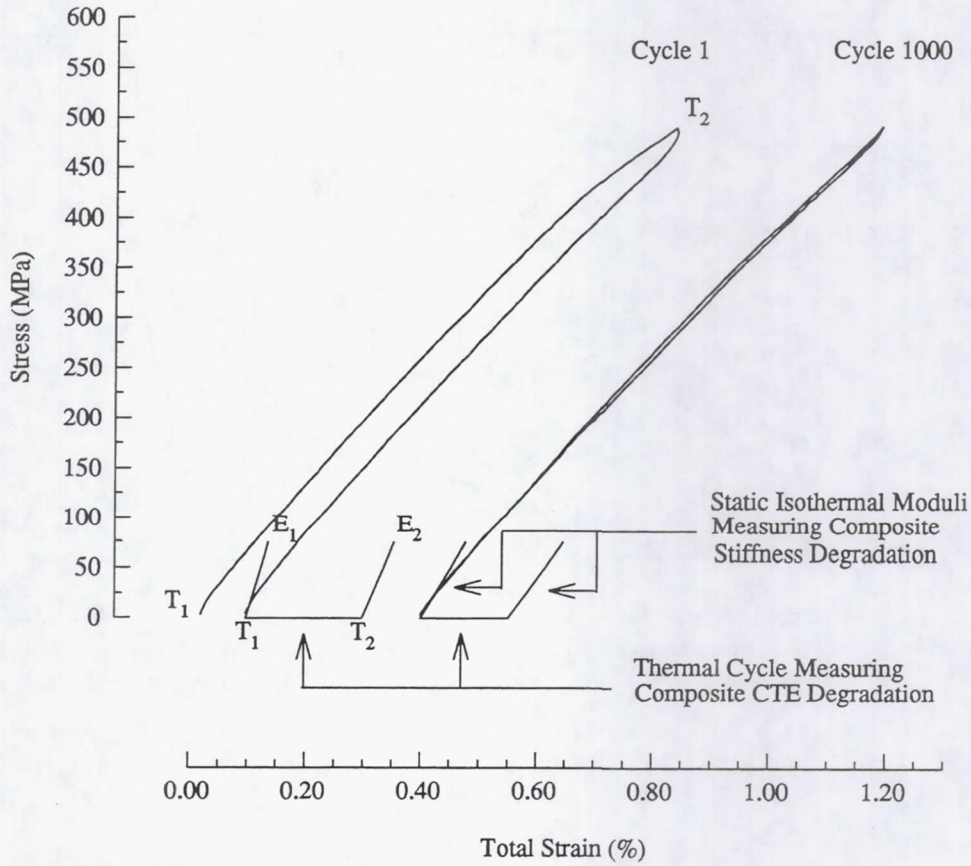

Figure 1.-Improved test methodology enabling definitive quantification of thermomechanical fatigue damage progression.

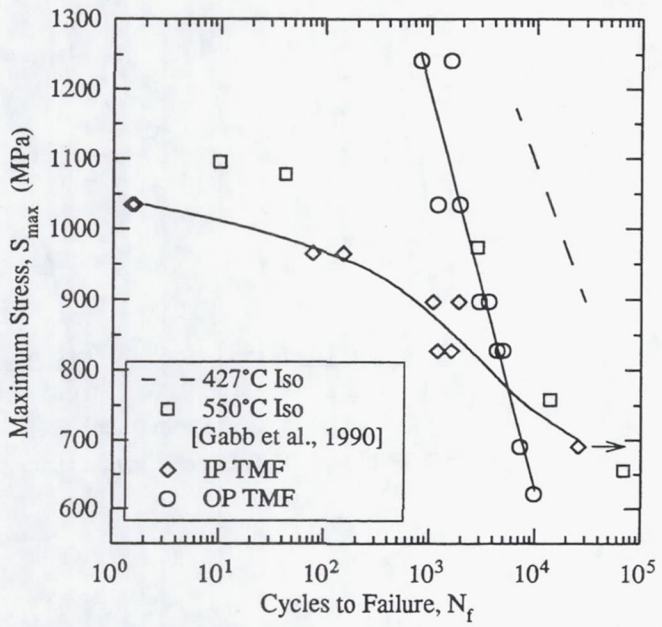

Figure 2. Stress-based fatigue life comparison for TMF of $[0]_9$ SCS-6/Ti-15-3 with a temperature cycle of 93-538°C.

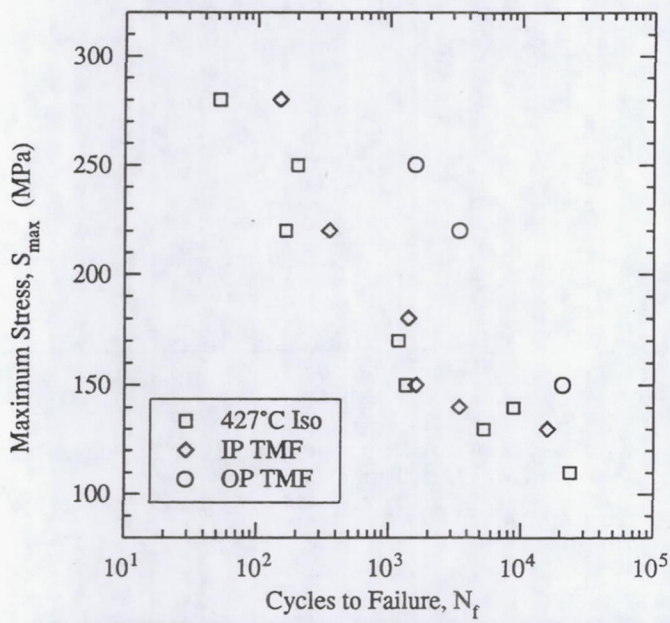

Figure 3. Stress-based fatigue life comparison for TMF of $[90]_8$ SCS-6/Ti-15-3 with a temperature cycle of 200-427°C.

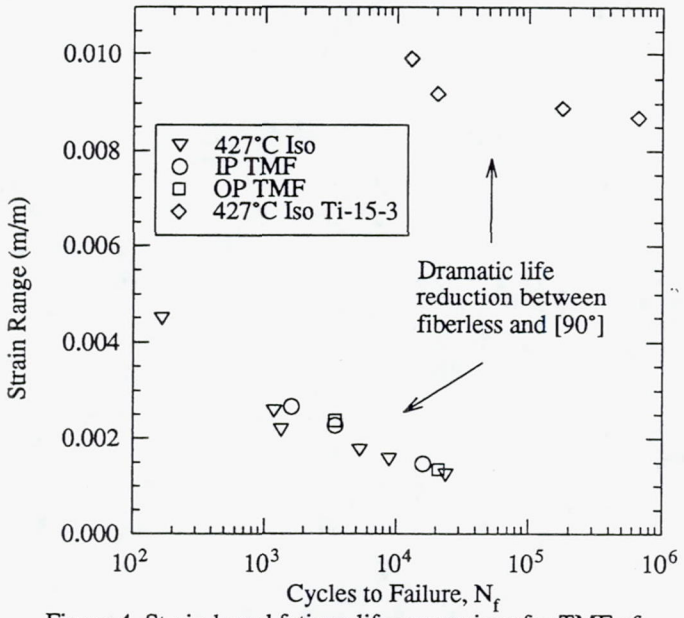

Figure 4. Strain-based fatigue life comparison for TMF of $[90]_8$ SCS-6/Ti-15-3 and fiberless Ti-15-3.

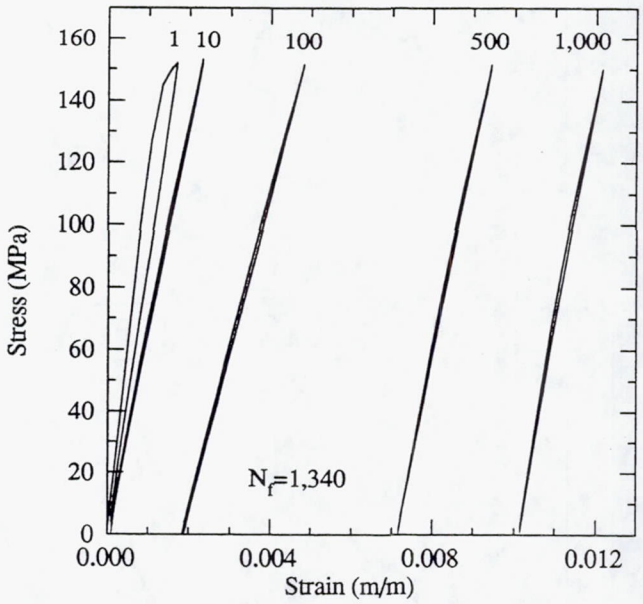

Figure 5. Isothermal deformation response of $[90]_8$ at 427°C with S_{max} = 150 MPa.

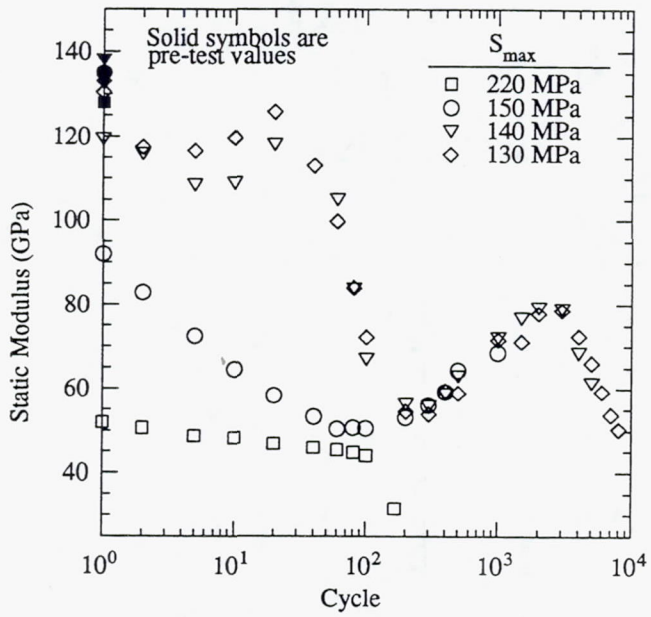

Figure 6. Degradation of the 427°C static modulus during 427°C isothermal fatigue.

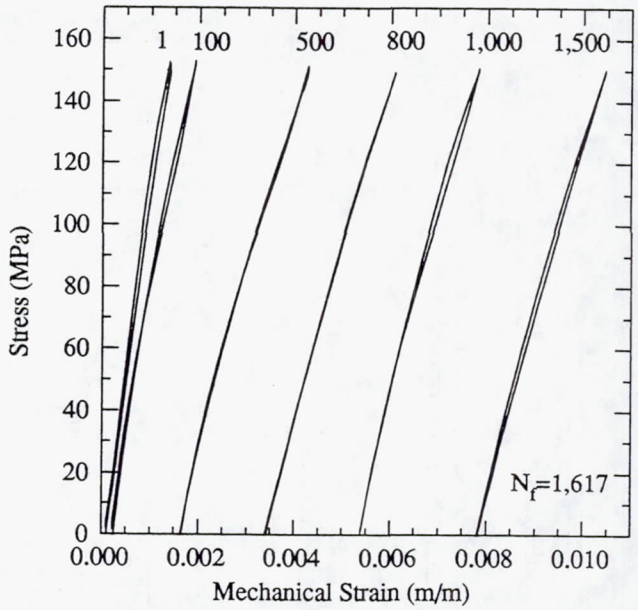

Figure 7. IP 200-427°C TMF deformation response with S_{max} = 150 MPa.

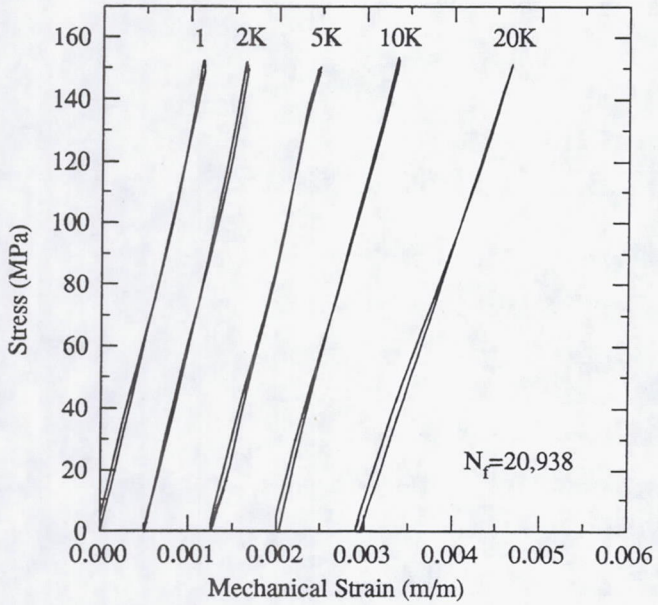

Figure 8. OP 200-427°C TMF deformation response with S_{max} = 150 MPa.

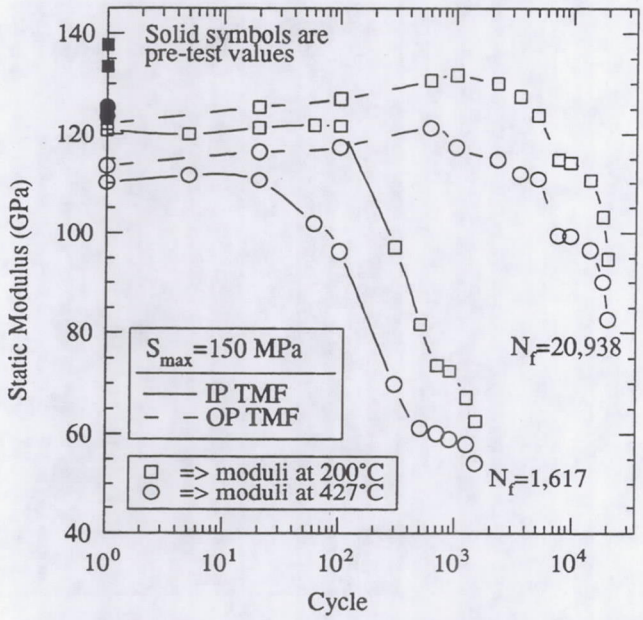

Figure 9. Degradation of the 200 and 427°C isothermal moduli during IP and OP TMF with a temperature cycle of 200-427°C.

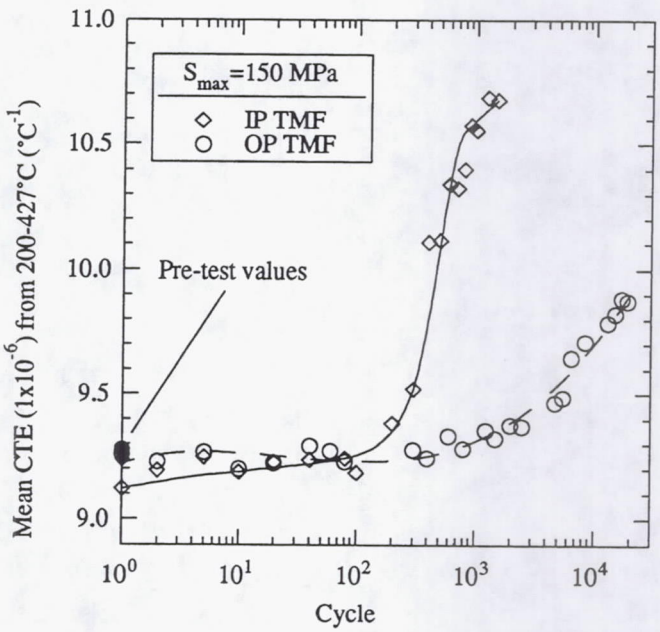

Figure 10. Degradation of the mean CTE during IP and OP TMF with a temperature cycle of 200-427°C.

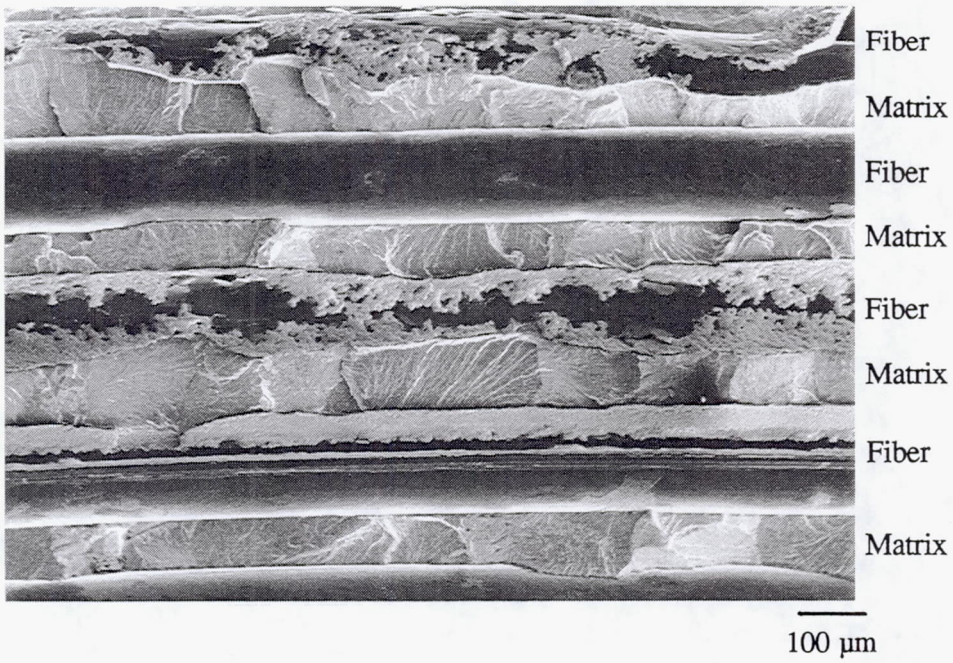

Figure 11. A SEM fractograph taken from an IP TMF test with S_{max} = 140 MPa showing extensive matrix cracking.

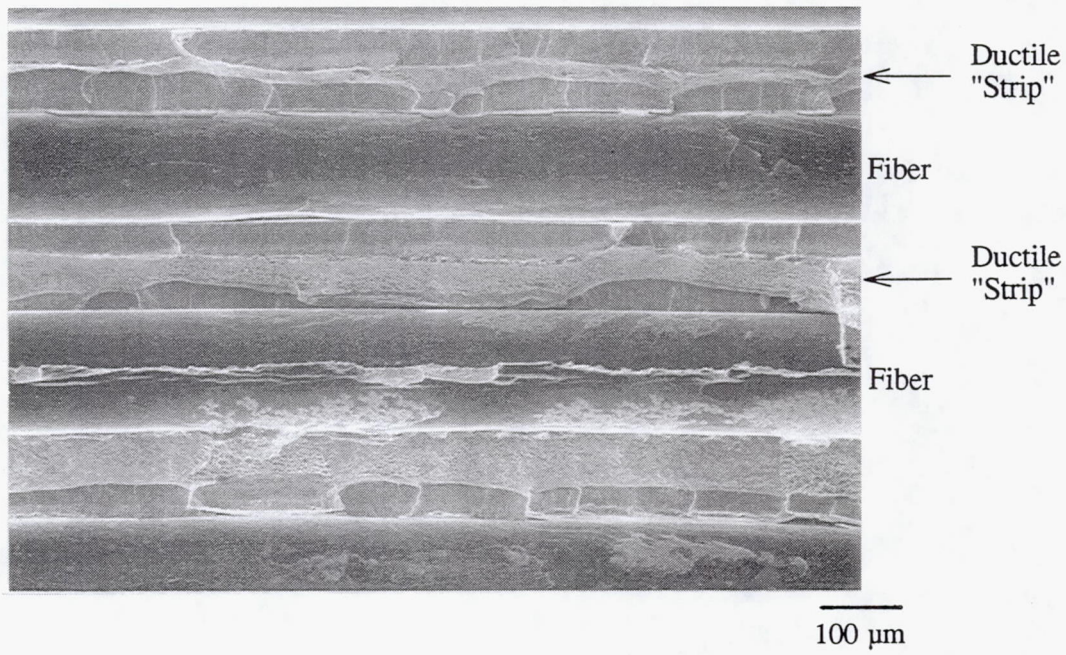

Figure 12. A SEM fractograph taken from an OP TMF test with S_{max} = 250 MPa showing ductile "strips" along matrix layer centerlines.

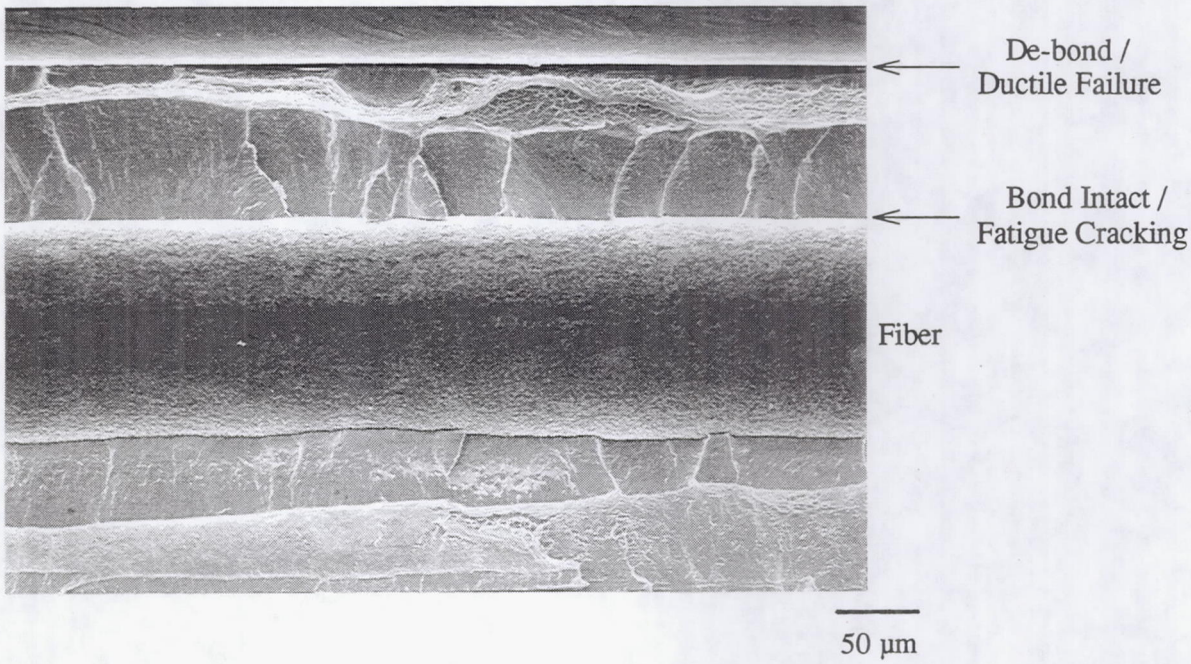

Figure 13. A SEM fractograph taken from an OP TMF test with S_{max} = 150 MPa showing an intact bond associated with fatigue cracking and a de-bond associated with ductile failure.

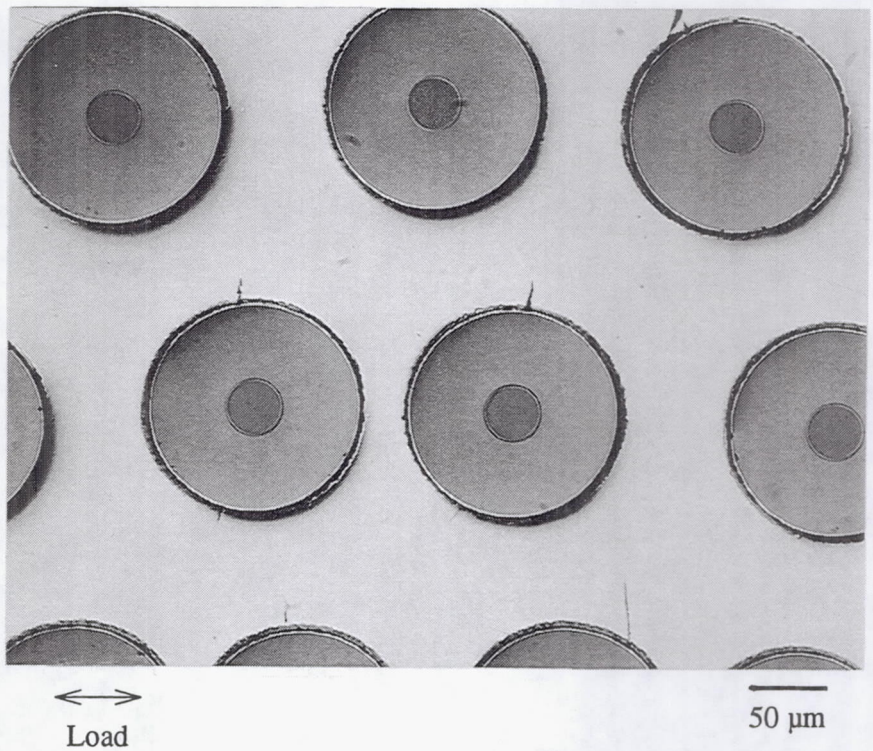

Figure 14. A metallographic section (longitudinal cut through the thickness) taken from an OP TMF test with S_{max} = 250 MPa.

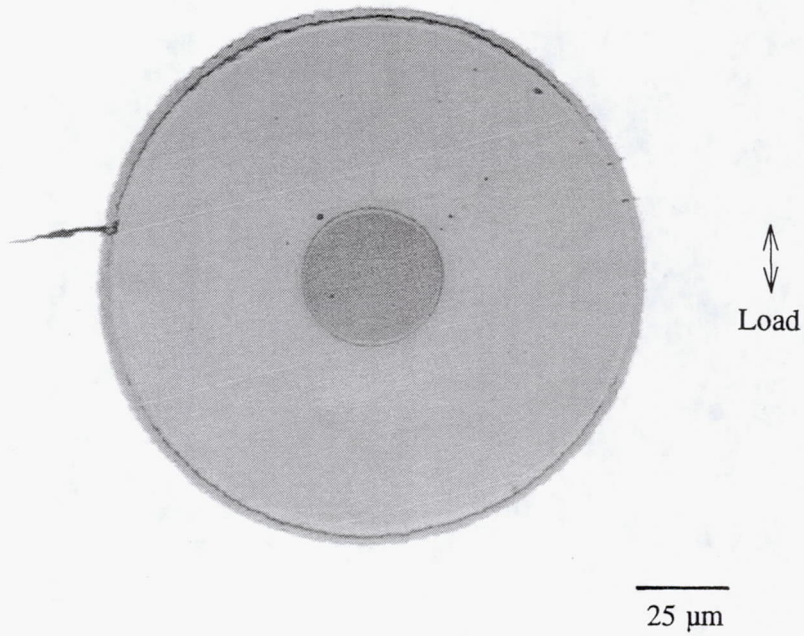

Figure 15. A metallographic section (longitudinal cut through the thickness) taken from an isothermal test with S_{max} = 130 MPa showing F/M de-bonding in the loading direction and intact bonds at the 9 (below crack) and 3 o'clock positions.

REPORT DOCUMENTATION PAGE

Form Approved
OMB No. 0704-0188

1. AGENCY USE ONLY (*Leave blank*)	2. REPORT DATE	3. REPORT TYPE AND DATES COVERED
	October 1993	Final Contractor Report

4. TITLE AND SUBTITLE

Thermomechanical and Isothermal Fatigue Behavior of a $[90]_8$ Titanium Matrix Composite

5. FUNDING NUMBERS

WU–510–01–50
C–NAS3–25266

6. AUTHOR(S)

Michael G. Castelli

7. PERFORMING ORGANIZATION NAME(S) AND ADDRESS(ES)

Sverdrup Technology, Inc.
Lewis Research Center Group
2001 Aerospace Parkway
Brook Park, Ohio 44142

8. PERFORMING ORGANIZATION REPORT NUMBER

E–8156

9. SPONSORING/MONITORING AGENCY NAME(S) AND ADDRESS(ES)

National Aeronautics and Space Administration
Lewis Research Center
Cleveland, Ohio 44135–3191

10. SPONSORING/MONITORING AGENCY REPORT NUMBER

NASA CR–191196

11. SUPPLEMENTARY NOTES

Project Manager, Rod Ellis, Structures Division, (216) 433–3340. Prepared for the Eighth Technical Conference on Composite Materials, sponsored by the American Society for Composites, Cleveland, Ohio, October 19–21, 1993.

12a. DISTRIBUTION/AVAILABILITY STATEMENT

Unclassified - Unlimited
Subject Category 24

12b. DISTRIBUTION CODE

13. ABSTRACT ***(Maximum 200 words)***

An experimental investigation was conducted to analyze the fatigue damage mechanisms operative in a 35 fiber volume percent [90°] titanium matrix composite (TMC) under 427°C isothermal and thermomechanical loading conditions. The thermomechanical fatigue (TMF) tests were performed with a temperature cycle from 200 to 427 °C under closely controlled conditions to define both the deformation and fatigue life behavior. Degradation of the TMC's isothermal elastic moduli and coefficient of thermal expansion were monitored throughout the TMF tests. The results indicated TMF life trends which contrasted those established in a comparable [0°] system, as TMF loading of the [90°] TMC was not found to be "life-limiting" in comparison to maximum temperature isothermal conditions. In-phase lives were very similar to those established under 427°C isothermal conditions. High stress isothermal fatigue at 427°C produced increased strain ratchetting and stiffness degradation relative to TMF conditions. Out-of-phase loadings produced TMF lives approximately an order of magnitude greater than the lives determined under isothermal and in-phase conditions. Extensive fractography and metallography were also performed. Two key issues were identified and appeared to dominate the fatigue damage and life of the [90°] TMC, namely, 1) the weak fiber/matrix interface, and 2) environmental attack of the fiber/matrix interface via the exposed [90°] fiber ends.

14. SUBJECT TERMS

Thermomechanical fatigue; Titanium matrix composites; SCS-6/Ti-15-3; Damage; Transversely reinforced composites

15. NUMBER OF PAGES
14

16. PRICE CODE
A03

17. SECURITY CLASSIFICATION OF REPORT	18. SECURITY CLASSIFICATION OF THIS PAGE	19. SECURITY CLASSIFICATION OF ABSTRACT	20. LIMITATION OF ABSTRACT
Unclassified	Unclassified	Unclassified	